






## Design and Implementation of a 300A Modular Welding Inverter

Cansu ÖZTÜRK YILMAZ<sup>1</sup> , Oğuz ŞİMŞEK<sup>2</sup> , M. Timur AYDEMİR<sup>3,\*</sup> 

<sup>1,3</sup>Gazi University, Faculty of Engineering, Dept. of Electrical and Electronic Eng. Ankara, TURKEY

<sup>2</sup>4Z Electronics Automation and Welding Systems, Ankara, TURKEY

### Article Info

Received: 03/04/2019

Accepted: 27/04/2019

### Keywords

Welding inverters,  
Dual forward converter,  
Series input parallel  
output converters,

### Abstract

Welding machines are one of the most important application areas of power electronics. Controlling the fast dynamics of these machines while keeping the efficiency high is a challenging task. Several topologies and control methods have been proposed in the literature. This paper presents a modular structure for a 9.6 kW welding inverter. The design process is explained in detail. Simulation and experimental results are provided to show that the proposed system can be a viable solution.

## 1. INTRODUCTION

Welding is an important industrial application area of power electronics. While it was dominated by transformer-based designs in the past, the situation has changed dramatically in the last two decades. Nowadays the situation is other way around since the raw materials such as steel and copper cost more now, power electronic semiconductors are cheaper and more readily available, and finally digital controllers can easily handle difficult tasks [1-2]. With the advent of semiconductors, the switching frequencies keep increasing causing reduction in the size of welding machines. However, increased frequencies also increase the switching losses and radiated EMI. There are papers in the literature suggesting different methods to alleviate these problems. One of the proposed solutions is to use modular systems. Modular AC-DC power converter structures with three-wire and four-wire were compared in [3]. It was concluded that the prior one has better power factor correction and harmonic content. The proposed structure utilized modified buck converters. Power factor correction stage is a requirement now in many countries. A PFC phase modulated resonant transition converter is presented in [4].

Resonant mode converters are widely used to reduce the switching losses [5]. The problem with resonant mode is that the current peaks are very high and the control is more complicated. Most of the welding inverters have two secondary windings. A topology with two current-doubler rectifiers proposed in [6]. The proposed topology has reduced conduction losses due to the lower inductor current, at the cost of increased size and cost. A novel method is proposed in [7] to control the bus voltage and to improve the power factor by utilizing pulsed currents.

This paper presents the design and implementation of a 300 A, 9.6 kW output welding inverter with modular structures. Each module has a dual-forward converter as these converters provide a safe and simple operation in terms of magnetic saturation and switching. In order to reduce the switch voltages, the primary terminals of the two transformers are connected in series while the secondary terminals are connected in parallel to share the load current. A closed loop controller is designed to keep the load current constant.

\*Corresponding author, e-mail: aydemirmt@gazi.edu.tr

The design steps of the converter power stage are described in Section 2. Both power and control designs are explained. Section 3 and 4 give the simulation and experimental results.

## 2. CONVERTER DESIGN

Modern welding machines utilize power electronic converters. Half-bridge, dual forward or full bridge converters are used depending on the power level. Some manufacturers prefer to use resonant mode operation for reduced losses at the cost of more complicated design. In this work dual forward converter has been used. The advantage of these converters is that the two switches are turned on and off simultaneously reducing the complexity of gate drives, and that the flux resetting of the transformer is achieved automatically. On the other hand, the flux of the transformer is unidirectional and this causes the transformer to be larger. The topology selected for this application is shown in Figure 1. As seen at the figure, there are two dual-forward converters with the inputs connected in series and the outputs connected in parallel. This structure allows the use of lower voltage MOSFETS and thus increased switching frequencies [8]. Other advantages are that the transformer turns ratios can be decreased, and the system can be designed for higher input voltages (i.e. operating from three-phase input).

Both converters operate in-phase, reflecting half of the bus voltage to their secondary windings when the switches are on. Energy is transferred to the load through the forward biased diodes. The maximum possible value of the duty cycle ratio is 50%, and when the switches are turned off the energy transfer ceases. The magnetizing current flows through the diodes of the primary resetting the flux before the end of the period. Meanwhile, the load current flows through the freewheeling diodes at the secondary windings of each converter.

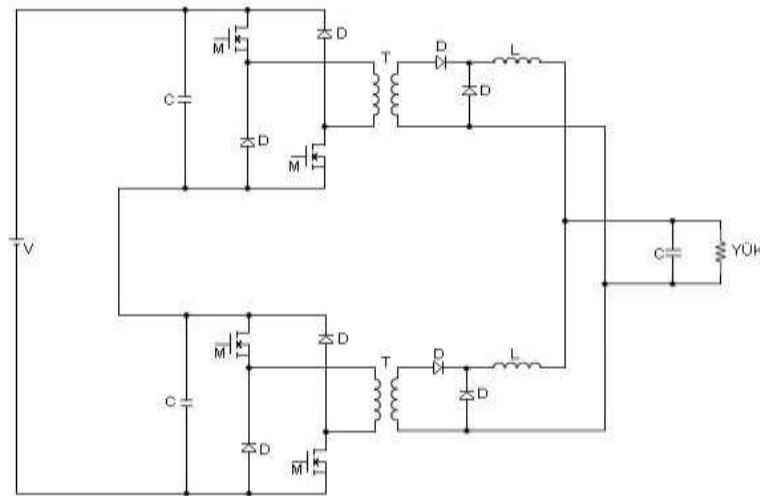


**Figure 1.** Series-Input Parallel-Output connected dual forward converter structure

Due to the parallel secondary structure, the load current is equal to the sum of the two transformer secondary currents. If all elements are identical and the switching is balanced, these currents are equal.

In the following sub-sections, the design steps of the converter are described for a 300 A welder. The supply is a three-phase 50 Hz AC source. The switching frequency is selected as 50 kHz, large enough to reduce the size and low enough for acceptable power losses.

### 2.1. Design of the Power Stage

The output voltage of the welding machine where the converter will be used and thus the lowest output power is defined by the international standard EN60974-1. Accordingly, the output voltage equation for a welding current of  $I_W = 300A$  is found as  $V_{arc} = I_W \times 0,04 + 20 = 32 V$ . This means that the welding power is 9.6 kW.

Considering the secondary rectifier voltage drop (1 V) and output shock and transmission drops (approximately 2 V), the lowest output voltage value in the transformer secondary side is calculated as 35 V. The power to be transferred to the secondary should be  $P_S = 300 \times 35 = 10.5$  kW. Based on these values the design parameters for each transformer are given in Table I.

Thickness of conductive skin at 50 kHz is  $\varepsilon = 66.2 \div \sqrt{50000} = 0.3$ .  $2\varepsilon$  thick foil conductors with a much higher filling ratio have been used for the windings. Core selection is realized based on the following equation;

$$W_a A_c = P_o J 10^4 / (4\eta B f K) \quad (1)$$

**Table 1. Design Data**

Minimum dc bus voltage	203 V
Maximum dc voltage	270 V
Output power	5250 W
Output voltage	50 V
Output current	150 A
Regulation	0.5%
Targeted efficiency	95%
Maximum duty cycle ratio	47%

where  $W_a A_c$  is the area product ( $m^4$ ),  $W_a$  is the window area,  $A_c$  is the core cross-section area,  $J$  is the current carrying capacity ( $A/m^2$ ),  $P_o$  is the power,  $B$  is the magnetic flux ( $Wb/m^2$ ),  $f$  is the switching frequency,  $K$  is the filling coefficient, and  $\eta$  is the efficiency. If  $J = 2.5$   $A/mm^2$  and  $K = 0.2$  are chosen the area product ( $W_a A_c$ ) is found to be  $25.58$   $cm^4$ . EE 6527 of Cosmo Ferrites has been selected as the core. The properties of the core are listed in Table II.

**Table 2. Properties of the selected core**

Magnetic material	CF139	Core cross-section area ( $cm^2$ )	5.3
Magnetic line length (mm)	147	Volume ( $mm^3$ )	78200
Window height (cm)	1.21	$A_L$ (nH)	8100
Window section ( $cm^2$ )	5.4	Average lap length (cm)	14
Area product ( $cm^4$ )	28.6		

Turn number of the primary winding can be calculated by using the following equation.

$$N_p = \frac{V_{in(\min)} d_{(max)}}{f A_c \Delta B} \quad (2)$$

If the saturation level is chosen as  $\Delta B = 0.3T$ , the turn number is found to be 12 for the given data. Transformer conversion rate is found as follows:

$$n = \frac{N_p}{N_s} = \frac{V_{in(\text{nominal})} * d_{(max)}}{V_{out}} = \frac{270 \times 0.47}{50} = 2.5$$

Then  $N_s$  is found as 4.8 and it is rounded up to 5 turns, changing the turns ratio to 2.4. Based on these numbers the primary and secondary coil inductance values are calculated as 1.17 mH and 202.5  $\mu$ H. The transformer has been wound with sandwich technique as primary/2-secondary-primary/2 as shown in Fig. 2. Nominal duty cycle value is found as 0.32 from the following equation.

$$d = n V_o / V_i^{nom} \quad (3)$$

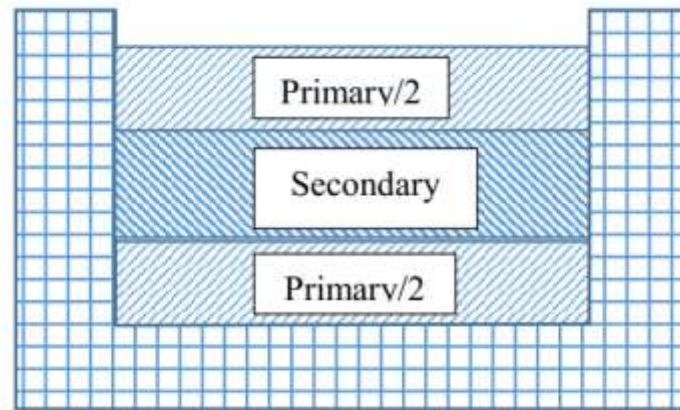


**Figure 2.** Sandwich winding structure of the transformer

The extreme values are found by using the minimum and maximum input voltages as 0.22 and 0.38. Based on these values the primary and secondary maximum rms currents are found as 38.5 and 61.6 A, respectively. Copper folio conductors have been used in the transformer. The thickness of the sheet is 0.33 mm for the primary. Two folio layers, each with a thickness of 0.3 mm, have been used in the secondary, with a layer of isolation in between.

Average length of turn for the primary is 14 cm. Therefore, the conductor length is 168 cm yielding 2.73 mΩ primary winding resistance and 4.88 W copper loss. Similar calculations result in 70 cm conductor length, 500.7 μΩ conductor resistance and 4.66 W power loss. Total copper loss is 9.54 W and as a result the regulation is

$$\alpha = P_{copper}/P_o = 0.18\% \quad (4)$$

which is better than the specified design value.

The core loss data of the core is given as 600 kW/m<sup>3</sup> in the data sheet for 50 kHz. Therefore, the core loss is 47 W, making the total power loss is around 57 W and the efficiency of the transformer is around 99%. The switch selection has been made as 650 V, 40 A FGH40N60UFD IGBT devices of Fairchild company. Two of these devices were paralleled for each switch. The switching energy of one device is given as 1.89 mJ at 400 V. Considering the operation voltage of the converters in this application is around 250 V, this energy can be scaled to 1.18 mJ. At 50 kHz switching frequency the switching loss is calculated as 59.1 W per switch (two devices in parallel). As there are two of them in one bridge and there are two bridges, total switching loss is 236.4 W. The on-state voltage of the devices is around 2.2 V, and with the 62.5 A primary current and 0.32 duty cycle ratio the conduction loss is around 44 W per switch, totaling to 176 W for the converters.

The flux-reset diodes have been selected as 600 V, 30 A STTH30R06 devices of ST. These devices have 1.1 V forward voltage drops. Considering that they carry only the magnetizing inductance, their power loss has not been calculated.

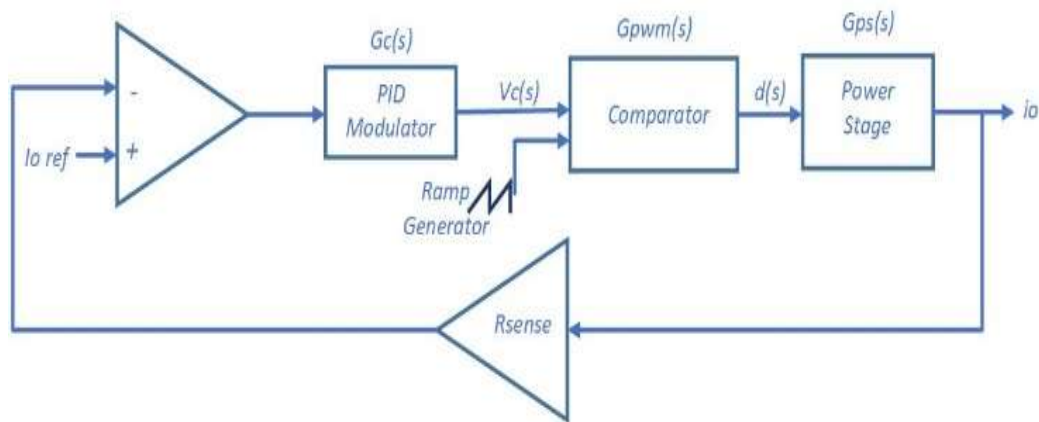
On the secondary diode selection was made as 60 A, 300 V ultrafast diodes FFA60UP30DN of Fairchild. These are modules including two diodes. Two of these modules are connected in parallel for the forward diode, and three of them connected in parallel for the freewheeling diode. Each diode has 1.5 V drop. This means at 150 A, there is a power loss of 225W total in each converter module. Since there are two secondary modules, total conduction loss is 450 W. The reverse recovery loss of these diodes are negligible. All the power loss values are summarized in Table III. The overall efficiency is estimated to be around 90.8%.

**Table 3.** Power losses of the converter

Transformer Loss (W)	114
IGBT Switching Loss (W)	236
IGBT Conduction Loss (W)	176
Secondary Diode Loss (W)	450
Total Loss (W)	976
Efficiency (%)	90.8

## 2.2. Controller Design

The feedback control design for the converters is described in this sub-section. The function of the controller is to keep the welding current constant and therefore a current controller needs to be designed. The controller structure is shown in Fig. 3.

**Figure 2.** Current control feedback structure

The current is sensed by a sense resistor and fed back. The open loop transfer function is found as follows:

$$G(s) = G_c(s)G_{pwm}(s)G_{ps}(s) \quad (5)$$

In (5),  $G_c(s)$  is the controller transfer function,  $G_{pwm}(s)$  is the transfer function of the PWM block, and  $G_{ps}(s)$  is the power stage transfer function. These functions are defined as follows:

$$G_c(s) = K_p + K_i/s \quad (6)$$

$$G_{pwm}(s) = d(s)/V_{sawtooth} \quad (7)$$

$$G_{ps}(s) = \frac{1}{n} \frac{1}{s^2 LC + s \frac{L}{R} + 1} \quad (8)$$

Calculations for a stable control system yield  $K_p = 6$  and  $K_i = 16504$ . The capacitor at the output is very small and could be ignored, reducing the system order to one.

## 3. SIMULATION RESULTS

The converter whose schematic is shown in Fig. 4 was simulated in LTSpice with the closed loop controller. In the simulation, a 540 V DC source is used at the input. 50 kHz switching pulses are sent to the switches of the two converters simultaneously. A resistor is connected as the load. The average value of the load voltage is expected to be approximately 32 V while the average value of the load current is expected to be approximately 300 A. As shown in Fig. 5, the currents through each inductors are 150A. In order to show the effectiveness of the controller, the load is decreased 50% after the steady state is reached. Fig. 6 shows the response.

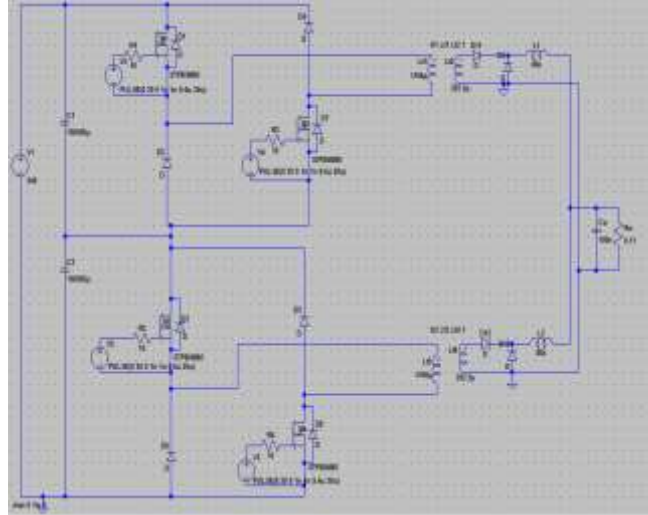


**Figure 4.** Simulated converter structure

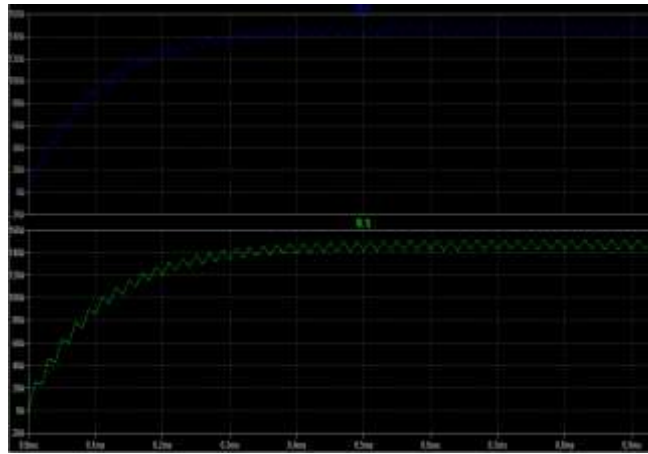


**Figure 5.** Inductor currents

A test was also performed to see the effect of unbalanced transformers. In the previous results the transformers have been assumed identical. Fig. 7 shows the response of the converter if the magnetizing inductance values ( $L_m$ ) of the transformers are 966 mH and 1066 mH respectively. As seen on the results, the current is shared equally in spite of the differences.

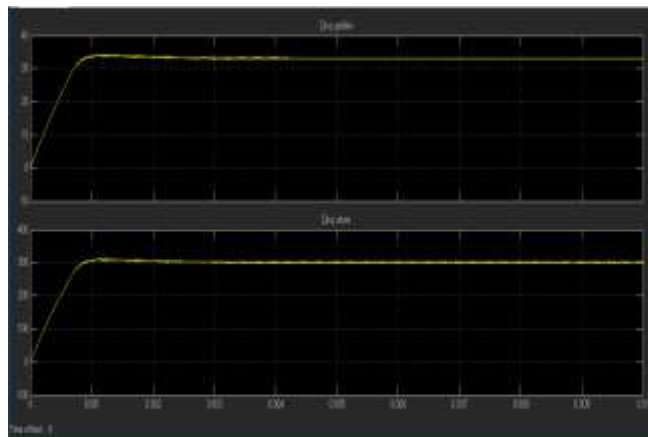


**Figure 6.** Response to load change (upper trace: load voltage, lower trace: inductor current).

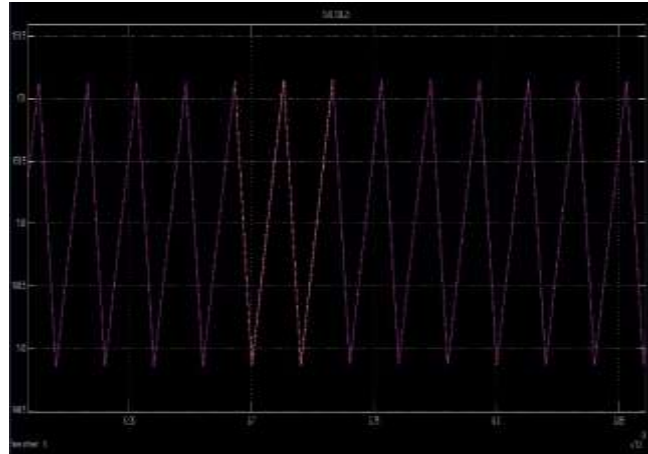


*Figure 7. Non-identical transformer response to inductor currents*

#### 4. EXPERIMENTAL RESULTS

The system was built and tested in the laboratory. The test set-up is shown in Fig. 8. Fig. 9 shows the operation at 300 A. Fig. 10 shows the current and voltage at MIG welding at 160 A load current. As seen from the graphs the converter response is as expected. The load current is shared between the two converters equally.

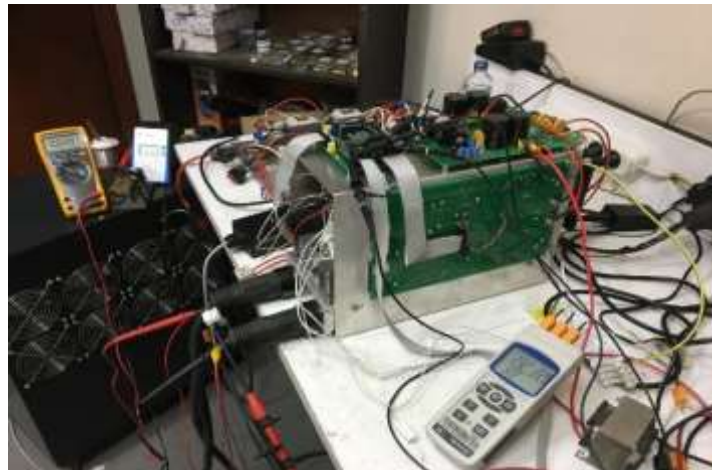


*Figure 8. Experimental set-up*

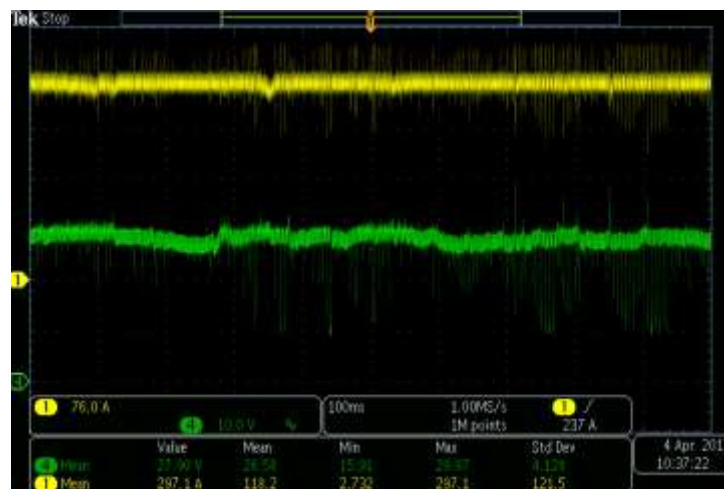


*Figure 9. Current (Ch. 1, upper trace) and voltage (Ch.4, lower trace) at 300 A.*

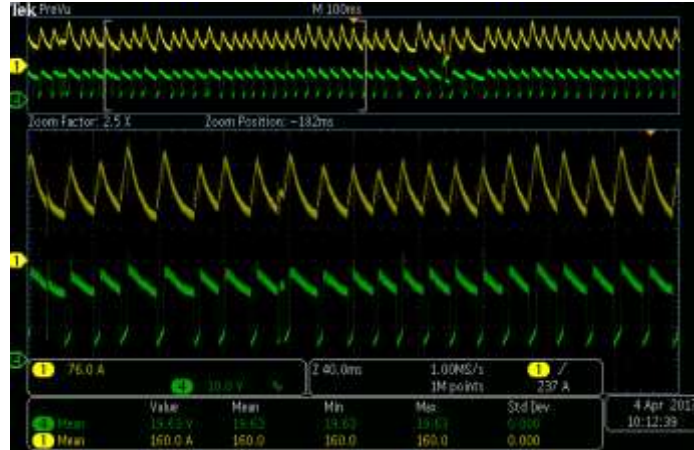


**Figure 10.** Current (Ch.1, lower trace) and the voltage (Ch. 4, upper trace); MIG operation at 160 A.

## 5. CONCLUSION

The design and implementation of a welding inverter utilizing two identical modules of dual-forward converters are described. The modules are connected in series at the primary side and in parallel at the secondary side. This allows the use of lower voltage devices and higher switching frequencies. A controller design is also given to obtain constant welding current. Simulation and experimental results show that the controller performance is good, the welding current can be adjusted as desired, and the current is shared among the modules even when there is a mismatch between the modules.

## ACKNOWLEDGMENT

This work has been supported by Turkish Ministry of Industry and Technology under the project grant number 0914.STZ.2015. The authors wish to thank for this support.

## CONFLICT OF INTEREST

No conflict of interest was declared by the authors

## REFERENCES

- [1] Zackiewicz, C. "DC-DC Power Converter Design for a Portable Affordable Welder System (PAWS)." Electronic Thesis or Dissertation. *Wright State University*, 2011. <https://etd.ohiolink.edu/>.
- [2] Paul, A.K. "Power electronics help reduce diversity of arc welding process for optimal performance", in *Proc. of Power Electronics, Drives and Energy Systems (PEDES) & 2010 Power India*, 2010, pp. 1-7.
- [3] Narula, S., Bhuvaneswari G. and Singh, B. "A modular converter for welding power supply with improved power quality," *2012 IEEE International Conference on Power Electronics, Drives and Energy Systems (PEDES)*, Bengaluru, 2012, pp. 1-4.
- [4] Kar, A., Nanda A., and Sengupta, M. "Design, analysis, fabrication and practical testing of a lab developed power converter prototype in electric arc welding," *2017 National Power Electronics Conference (NPEC)*, Pune, 2017, pp. 123-128.
- [5] Navarro-Crespin, A. Casanueva, R., Azcondo, F. J. "Performance improvements in an arc-welding power supply based on resonant inverters", *IEEE Trans. Ind. Appl.*, 48(3), 888-894 (2012).



- [6] Wang, J.M., Wu, S.T. "A Novel Inverter for Arc Welding Machines", *IEEE Trans. Ind. Electron.*, 62(3) 1431-1439 (2015).
- [7] Bellec, Q., Le Claire, J., Benkhoris M. F. and Coulibaly, P. "Power factor correction and DC voltage control limits for arc welding application using pulsed current," *IECON 2018-44th Annual Conference of the IEEE Industrial Electronics Society*, Washington, DC, 2018, pp. 1406-1411.
- [8] Ayyanar, R., Giri, R., Mohan, N., "Active Input–Voltage and Load–Current Sharing in Input-Series and Output-Parallel Connected Modular DC–DC Converters Using Dynamic Input-Voltage Reference Scheme" *IEEE Tran. on Power Elec.*, 19(6) 1462-1473 (2004).